CSIRO PUBLISHING
Functional Plant Biology, 2018, **45**, 362–377
https://doi.org/10.1071/FP17225

Simulating daily field crop canopy photosynthesis: an integrated software package

Alex Wu[A,C,D], *Al Doherty*[A,C], *Graham D. Farquhar*[B,C] *and Graeme L. Hammer*[A,C]

[A]Centre for Plant Science, Queensland Alliance for Agriculture and Food Innovation, The University of Queensland, Brisbane, Qld 4072, Australia.
[B]Research School of Biology, Australian National University, Canberra, ACT 2601, Australia.
[C]ARC Centre of Excellence for Translational Photosynthesis, Australia.
[D]Corresponding author. Email: c.wu1@uq.edu.au

Abstract. Photosynthetic manipulation is seen as a promising avenue for advancing field crop productivity. However, progress is constrained by the lack of connection between leaf-level photosynthetic manipulation and crop performance. Here we report on the development of a model of diurnal canopy photosynthesis for well watered conditions by using biochemical models of C_3 and C_4 photosynthesis upscaled to the canopy level using the simple and robust sun–shade leaves representation of the canopy. The canopy model was integrated over the time course of the day for diurnal canopy photosynthesis simulation. Rationality analysis of the model showed that it simulated the expected responses in diurnal canopy photosynthesis and daily biomass accumulation to key environmental factors (i.e. radiation, temperature and CO_2), canopy attributes (e.g. leaf area index and leaf angle) and canopy nitrogen status (i.e. specific leaf nitrogen and its profile through the canopy). This Diurnal Canopy Photosynthesis Simulator (DCaPS) was developed into a web-based application to enhance usability of the model. Applications of the DCaPS package for assessing likely canopy-level consequences of changes in photosynthetic properties and its implications for connecting photosynthesis with crop growth and development modelling are discussed.

Additional keywords: CO_2 partial pressure, dry matter accumulation, modeling, modelling, radiation, temperature effects.

Received 9 August 2017, accepted 29 September 2017, published online 13 November 2017

Introduction

The next advance in field crop productivity will likely need to come from improving crop use efficiency of resources (e.g. radiation, CO_2, water and nitrogen), aspects of which are closely linked with overall crop photosynthetic efficiency (Long *et al*. 2015). For this, there is an emerging agenda focussed on genetic manipulation of the biochemical pathway of photosynthesis aiming to enhance photosynthesis for improved crop yield (Evans 2013; Long *et al*. 2015). However, progress is limited by the lack of connection between biochemical/leaf-level photosynthetic manipulation and crop performance, which is influenced by interactions between (photosynthetic) genetic controls, plant growth and development processes, and environmental effects. Crop models that can incorporate the interactions and integrate across scales of biological organisation might be the tool needed to accelerate progress in photosynthetic enhancement (Wu *et al*. 2016).

In many crop models that are used for seasonal simulation of crop growth, development and yield, daily biomass accumulation (which is determined by canopy photosynthesis) is a key driver of crop growth that has been used to simulate source-limited plant growth. Canopy photosynthesis modelling began with empirical models of leaf photosynthetic light response (PLR), which were upscaled and integrated to simulate diurnal canopy photosynthesis (Monsi and Saeki 1953; Hammer *et al*. 2009). There are multiple approaches for such upscaling, which focussed on modelling the heterogeneous light environment within the canopy. These can be classified into models with 'simplified' canopy representation, such as multi-layer models (each layer partitioned into sunlit and shade leaf fractions) (Duncan *et al*. 1967), single-layer big-leaf models (Sellers *et al*. 1992; Sands 1995) or (single-layer) sun–shade leaves models (Hammer and Wright 1994; de Pury and Farquhar 1997). Another type of approach is detailed models, such as static 3D and dynamic 3D (Vos *et al*. 2010) canopy architecture models. The respective (dis)advantages of these models have been discussed (Wu *et al*. 2016) and many have supported the simplicity and robustness of the sun–shade leaves approach. This approach can use either single or multiple layers with canopy leaf area index in each layer(s) partitioned into sunlit and shade leaf fractions. Another widely used type of canopy photosynthesis simulation, which avoids the need for photosynthesis modelling and upscaling, is to utilise a simple empirical linear relationship between daily crop (aboveground) biomass increment and intercepted solar radiation (or radiation use efficiency, RUE) (Sinclair and Muchow 1999). Theoretical derivations have shown consistencies between the PLR and RUE approaches to modelling (Hammer and Wright 1994). Both types underpin source-limited plant growth simulation, which can be connected with crop models that incorporate both source- and sink-limited crop growth (Hammer *et al*. 2010). For example, the APSIM crop models (Hammer *et al*. 2009) provide important effects that can regulate canopy photosynthesis via crop nitrogen status, which influences photosynthetic capacity. This is an effective and robust framework for connecting photosynthesis with crop growth, development and yield simulation (Wu *et al*. 2016).

Given the focus of photosynthetic enhancement at the biochemical level for field crop improvement, the PLR and RUE types of canopy photosynthesis modelling may not be adequate despite their apparent success in crop models. Their responses to variations at the biochemical level and to environment are difficult to predict due to the aggregated nature of the models. To overcome the limitations, canopy models based on more mechanistic photosynthesis models (e.g. C_3 and C_4 photosynthesis models; von Caemmerer 2000) have emerged (de Pury and Farquhar 1997) and have been incorporated into vegetation growth models (e.g. BioCro, http://biocro.r-forge.r-project.org/, accessed 16 October 2017; Ecosys, http://ecosys.ualberta.ca/, accessed 16 October 2017; GECROS, Yin and van Laar (2005); and WIMOVAC, Humphries and Long (1995)). Most of these have utilised the simple and robust sun–shade leaves approach. However, there are only a limited number of such canopy photosynthesis models being applied in crop models (Yin and Struik 2008). Despite a limited number, these examples of modelling work demonstrated the value of using biochemical based canopy photosynthesis models to expand the biological functionality of crop models, which could potentially aid progress in photosynthetic enhancement for field crop improvement.

Besides the eventual target of incorporating diurnal canopy photosynthesis into field crop performance prediction, there is also a need for developing a standalone diurnal canopy photosynthesis simulator. This is likely to stimulate and guide different approaches to leaf-level photosynthesis research and reinforces thinking at the canopy level. For example, correlating Rubisco carboxylation rate with leaf nitrogen content would be useful for simulation of instantaneous canopy photosynthetic rate (de Pury and Farquhar 1997). More examples of relationships between photosynthetic and plant attributes have also emerged (Braune *et al*. 2009). As discussed above, there are existing examples of canopy models; however, they have been developed as integrated modules in more extensive vegetation growth models. A standalone diurnal canopy photosynthesis simulator that informs canopy CO_2 assimilation/biomass accumulation in terms of photosynthetic attributes and diurnal environment would be a desirable tool. Such a tool can be utilised to aid the wider community of photosynthesis experimentalists to understand consequences at a higher level over a longer simulation period, as well as providing a valuable teaching tool.

The rationale of extending crop modelling and aiding progress in photosynthesis research warrant the development for a standalone tool of diurnal canopy photosynthesis simulation. It will need to incorporate the biochemical models of photosynthesis as well as respond to diurnal environment effects for simulating canopy CO_2 assimilation/biomass accumulation of a field crop over a day. To develop such a tool, three objectives have been identified:

(1) develop a standalone C_3 and C_4 Diurnal Canopy Photosynthesis Simulator (DCaPS) for both C_3 and C_4 photosynthesis based on the concept of a cross-scale modelling framework that facilitates connection with crop growth and development dynamics (Wu *et al*. 2016),
(2) present model rationality tests by simulating responses to key environmental factors (i.e. light, CO_2 and temperature), canopy nitrogen status (i.e. specific leaf nitrogen and its profile through the canopy), and canopy attributes and architecture (i.e. canopy leaf area index and leaf angle), and
(3) develop DCaPS into an interactive web-based application that can be accessed using internet browsers on any major platform for simulating likely canopy-level consequences of photosynthetic changes.

The implications of the DCaPS package for crop modelling and it applications for photosynthetic manipulation are also discussed.

Model overview

The Diurnal Canopy Photosynthesis Simulator (DCaPS) calculates diurnal (period from sunrise to sunset) canopy CO_2 assimilation and daily (24 h) biomass increment for a crop under well watered conditions. A schematic diagram of the model is provided in Fig. 1, model detail in the next section, and a comprehensive description and list of model equations and parameters in Tables 1, 2 and the appendices. Daily values of incident solar radiation, air temperature (T_a) and air vapour pressure deficit (VPD_a), commonly used in crop models, were used to derive instantaneous values at the start of each hour over the diurnal period. A single-layer sunlit and shade leaf modelling approach was used. Canopy leaf area index (LAI_{can}) was partitioned into sunlit and shade leaf fractions using the sun–shade leaves modelling approach (Hammer and Wright 1994; de Pury and Farquhar 1997) to calculate the amount of photosynthetically active radiation (PAR) absorbed by each fraction. T_a was assumed as a proxy for leaf temperature (T_l), which affects photosynthetic physiology. The canopy profile of leaf nitrogen on a leaf area basis (specific leaf nitrogen, SLN) was input and used to calculate the maximum rate of Rubisco carboxylation (V_{cmax}), the maximum rate of electron transport (J_{max}) and the maximum phosphoenolpyruvate (PEP) carboxylase activity (V_{pmax}) (de Pury and Farquhar 1997), which are parameters of the C_3 and C_4 photosynthesis models (Farquhar *et al*. 1980; von Caemmerer 2000) used in DCaPS. The photosynthesis models were coupled with a CO_2 diffusion model to calculate C_c and CO_2 assimilation rate. Photosynthesis of both the sunlit and shade leaf fractions of the canopy were calculated, summed for the canopy, integrated hourly, and summed over the diurnal period to calculate total diurnal canopy photosynthesis, which was taken as the daily sum. This was converted to daily total biomass increment ($BIO_{total,DAY}$) assuming a conversion ratio (B), which combines factors allowing for biochemical conversion and maintenance respiration (Sinclair and Horie 1989). A fraction of $BIO_{total,DAY}$ was partitioned to root and

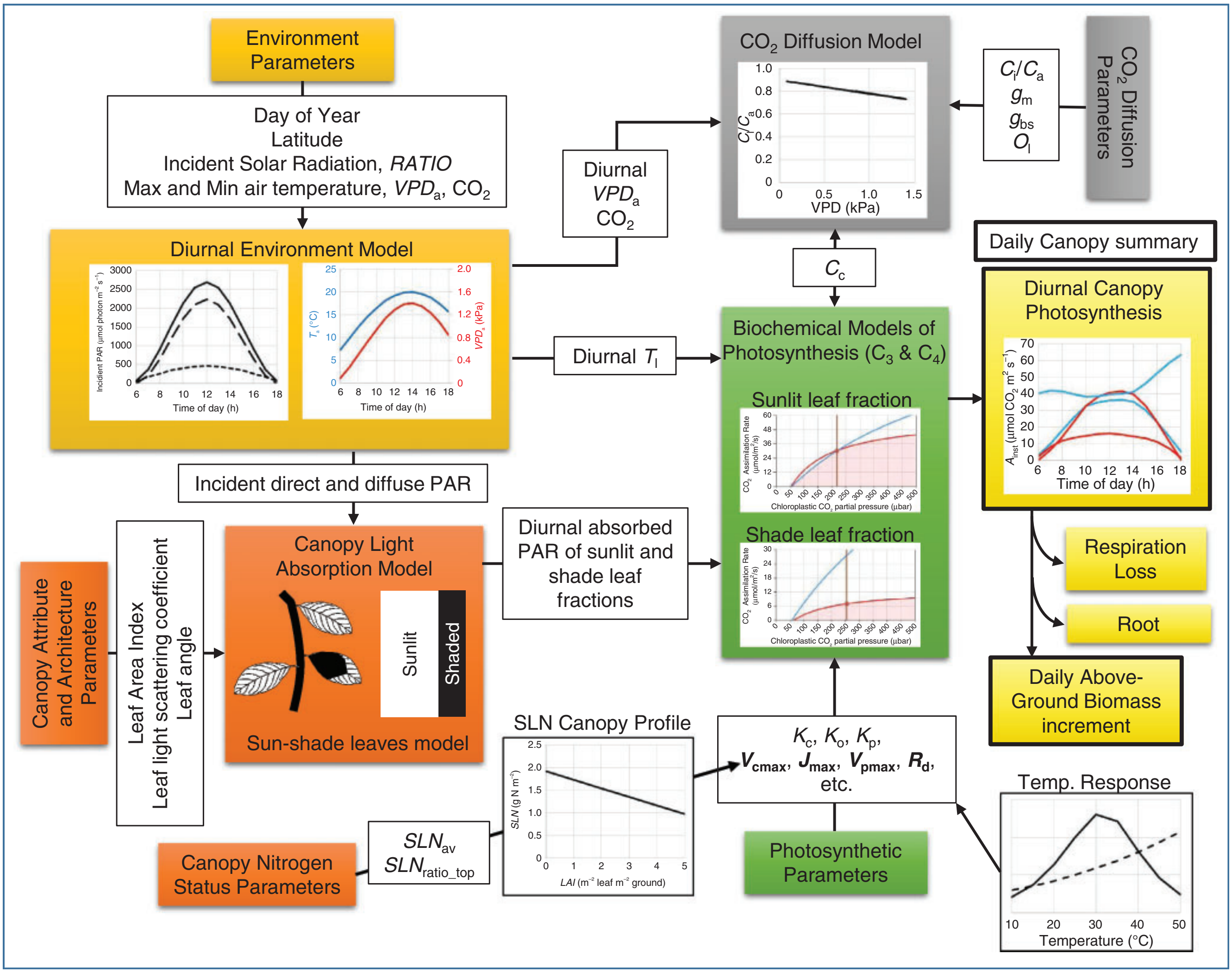

Fig. 1. Schematic of the Diurnal Canopy Photosynthesis Simulator (DCaPS). Model inputs are categorised into environment, canopy attributes and architecture, canopy nitrogen status, CO_2 diffusion, photosynthetic and temperature response parameters. Model outputs are diurnal environment variables, diurnal canopy photosynthesis and daily aboveground canopy biomass increment. The two-way arrow between the CO_2 diffusion model and the biochemical models indicates that the models are coupled and solved simultaneously for the chloroplastic CO_2 partial pressure (C_c) and photosynthesis. Parameters in bold font are driven by specific leaf nitrogen (SLN). Abbreviations: RATIO, atmospheric transmission ratio for incident solar radiation; VPD_a, air vapour pressure deficit; PAR, photosynthetic active radiation; SLN_{av}, canopy-average specific leaf nitrogen; SLN_{ratio_top}, ratio of SLN at the top of canopy to SLN_{av}; T_l, leaf temperature; g_m, mesophyll conductance for CO_2; g_{bs}, bundle-sheath conductance for CO_2; O_l, O_2 partial pressure inside leaves. The SLN canopy profile is used to calculate parameters in bold font. Comprehensive lists of the photosynthetic parameters are given in Tables 1, 2.

the remaining amount was taken as the daily aboveground canopy (shoot) biomass increment ($BIO_{shoot,DAY}$).

Model detail

Absorbed photosynthetically active radiation (PAR)

In both the C_3 and C_4 photosynthesis models (not replicated here, but see Appendix 1 and 2, available as Supplementary Material to this paper), the potential electron transport rates (J, µmol e$^-$ m^{-2} s^{-1}) of sunlit and shade leaf fractions are driven by absorbed PAR using a non-rectangular hyperbolic function (von Caemmerer 2000). Absorbed PAR for each of the sunlit and shade leaf fractions varies diurnally and its calculation requires diurnal total incident solar radiation, LAI_{can}, canopy architecture (in the form of canopy-average leaf angle), and optical properties (reflectance and transmittance) of leaves. Separation of absorbed PAR for the sunlit and shade leaf fractions of the canopy is a necessary detail to avoid errors in over estimation of photosynthetic rate (de Pury and Farquhar 1997).

The calculation of diurnal absorbed PAR depends on the radiation environment (Hammer and Wright 1994). First, diurnal extra-terrestrial radiation (S_o, MJ m^{-2} ground day^{-1}) was calculated from latitude (Lat, radians) and day of year (DAY) (Eqn A5, see Supplementary Material). Then diurnal total incident solar radiation on the ground (S_g, MJ m^{-2} ground s^{-1})

Table 1. Description of symbols used in the Diurnal Canopy Photosynthesis Simulator (DCaPS)

Symbol	Description	Units	Value and reference	Equation
		Daily canopy summary		
$A_{can,inst}$	Instantaneous canopy CO_2 assimilation[F]	µmol CO_2 m^{-2} ground s^{-1}	–	A73
$A_{can,DAY}$	Diurnal canopy CO_2 assimilation[F]	µmol CO_2 m^{-2} ground day^{-1}	–	A73
B	Conversion ratio combines factors allowing for biochemical conversion and maintenance respiration[A]	g biomass (g CO_2)$^{-1}$	0.41 (wheat and sorghum) (Sinclair and Horie 1989)	A74
$BIO_{total,DAY}$	Daily total biomass increment[F]	g biomass m^{-2} ground day^{-1}	–	A74
P_{shoot}	Fraction of aboveground (shoot) biomass to the total (shoot + root)[A,C]	g shoot biomass (g total biomass)$^{-1}$	–	A74
$BIO_{shoot,DAY}$	Daily aboveground canopy (shoot) biomass increment[C,E,F]	g biomass m^{-2} ground day^{-1}	–	A74
k_{DAY}	Canopy solar radiation extinction coefficient on daily basis[F]		–	A78
RAD_{DAY}	Total daily intercepted solar radiation[F]	MJ m^{-2} ground day^{-1}	–	A76
RUE_{DAY}	Radiation use efficiency on daily basis[F]	g biomass MJ^{-1}	–	A75
		Environmental parameters		
S_o	Total daily extra-terrestrial solar radiation[F]	MJ m^{-2} ground day^{-1}	–	A5
S_g	Total daily incident solar radiation[C,F]	MJ m^{-2} ground day^{-1}	–	A4
RATIO	Atmospheric transmission ratio[A,C]		–	A4
sc	Solar constant[A]	J m^{-2} ground s^{-1}	1360	A5
Lat	Latitude in radians (negative in the southern hemisphere)[A]	radians	–	A5
Rl	Radius vector[F]	radians	–	A6
Dl	Solar declination[F]	radians	–	A8
Wl°	Sunset hour-angle[F]	°	–	A7
Ll	Day length[F]	hr	–	A10
DAY	Day of year[A,C]		–	
t_{frac}	t as a fraction of Ll[F]		–	A12
$t_{sunrise}$	Time of sunrise[F]	hr	–	A13
t_{sunset}	Time of sunset[F]	hr	–	A14
α_{sun}	Angle of solar elevation[F]	radians or degree	–	A9
T_a	Air temperature[F]	°C	–	A15
$T_{a,max}$	Maximum T_a of DAY[A,C]	°C	–	A15
$T_{a,min}$	Minimum T_a of DAY[A,C]	°C	–	A15
m	Amount of time since time of minimum temperature[F]	hr	–	A15
n	Amount of time since t_{sunset}[F]	hr	–	A15
x_{lag}	Lag coefficient for the maximum temperature from $t_{sunrise}$[A]		1.8 (Parton and Logan 1981)	A15
y_{lag}	Lag coefficient for the night-time temperature from $t_{sunrise}$[A]		2.2 (Parton and Logan 1981)	A15
z_{lag}	Lag coefficient for the minimum temperature from $t_{sunrise}$[A]		1 (parameterised with hourly temperature data at Gatton, Australia)	A15
VPD_a	Air vapour pressure deficit[F]	kPa	–	A16
C_a	Air CO_2 partial pressure[A]	µbar	400	
O_a	Air O_2 partial pressure[A]	µbar	210 000	
I_o	Total incident solar radiation[F]	MJ m^{-2} ground s^{-1}	–	A3
I_{dir}	Incident direct radiation[F]	MJ m^{-2} ground s^{-1}	–	A2
I_{dif}	Incident diffuse radiation[F]	MJ m^{-2} ground s^{-1}	–	A1
I_{o_PAR}	Total incident photosynthetic active radiation[F]	µmol PAR m^{-2} ground s^{-1}	$I_{dir,PAR} + I_{dif,PAR}$	
I_{dir_PAR}	Direct incident photosynthetic active radiation[F]	µmol PAR m^{-2} ground s^{-1}	–	A21
I_{dif_PAR}	Diffuse incident photosynthetic active radiation[F]	µmol PAR m^{-2} ground s^{-1}	–	A22
$I_{abs,can}$	Absorbed PAR by the canopy[F]	µmol PAR m^{-2} ground s^{-1}	–	A23
$I_{abs,sun}$	Absorbed PAR by the sunlit fraction of the canopy[F]	µmol PAR m^{-2} ground s^{-1}	–	A31

(*continued next page*)

Table 1. (*continued*)

Symbol	Description	Units	Value and reference	Equation
$I_{abs,sh}$	Absorbed PAR by the shaded fraction of the canopy[F]	µmol PAR m^{-2} ground s^{-1}	–	A32
		Canopy attribute and architecture parameters		
LAI_{can}	Canopy leaf area index[A,C]	m^2 leaf m^{-2} ground	–	A20
LAI_{sun}	LAI of the sunlit leaf fraction[F]	m^2 leaf m^{-2} ground	–	A19
LAI_{sh}	LAI of the shade leaf fraction[F]	m^2 leaf m^{-2} ground	–	A20
L	Cumulative LAI from the top of canopy[F]	m^2 leaf m^{-2} ground	–	
k_b'	Direct and scattered direct PAR extinction coefficient[F]		–	A24
k_d'	Diffuse and scattered diffuse PAR extinction coefficient[F]		–	A24
k_b	Direct radiation extinction coefficient[F]		–	A25
k_d	Diffuse PAR extinction coefficient[A]		0.78 (de Pury and Farquhar 1997)	
σ	Leaf-level scattering coefficient for PAR[A]		0.15 (de Pury and Farquhar 1997)	
ρ_{cb}	Canopy-level reflection coefficient for direct PAR[F]		–	A29
ρ_{cd}	Canopy-level reflection coefficient for diffuse PAR[A]		0.036 (de Pury and Farquhar 1997)	
G	Leaf shadow projection coefficient[F]		–	A27
β	Canopy-average leaf inclination relative to the horizontal[A]	radians	60° (spherical leaf angle distribution) (de Pury and Farquhar 1997)	A27
T_l	Leaf temperature[A]	°C	T_a	1, 2
		Canopy nitrogen status parameters		
SLN_{av}	Specific leaf nitrogen averaged over the whole canopy[A,C]	g N m^{-2} leaf	1.45 (wheat) (de Pury and Farquhar 1997), 1.36 (sorghum) (van Oosterom *et al.* 2010)	A33
SLN_{ratio_top}	Ratio of SLN_o to SLN_{av}[A]	g N m^{-2} leaf	1.32 (wheat) (de Pury and Farquhar 1997), 1.30 (sorghum) (van Oosterom *et al.* 2010)	A33
SLN_o	SLN at the top of canopy[F]	g N m^{-2} leaf	–	A33
$N(L)$	SLN at L[F]	mmol N m^{-2} leaf	–	A34
N_o	SLN at the top of canopy[F]	mmol N m^{-2} leaf	–	A33
N_b	Base SLN at or below which leaf photosynthesis = 0[A]	mmol N m^{-2} leaf	25 (wheat) (de Pury and Farquhar 1997), 14 (sorghum) (Sinclair and Horie 1989)	A34
k_n	Coefficient of nitrogen allocation through canopy[F]		–	A36
		Photosynthesis parameters		
χ_V	Slope of linear relationship between V_{max} per leaf are at 25°C and N[B]	µmol CO_2 $mmol^{-1}$ N s^{-1}	1.16 (de Pury and Farquhar 1997) (wheat), 0.35 (sorghum) (Massad *et al.* 2007)	A37
χ_J	Slope of linear relationship between J_{max} per leaf are at 25°C and N[B]	µmol CO_2 $mmol^{-1}$ N s^{-1}	2.4 (wheat) (de Pury and Farquhar 1997), 2.4 (sorghum) (Massad *et al.* 2007)	A38
χ_R	Slope of linear relationship between R_d per leaf are at 25°C and N[F]	µmol CO_2 $mmol^{-1}$ N s^{-1}	$0.01\chi_V$ (wheat) (de Pury and Farquhar 1997), 0 (sorghum) (Massad *et al.* 2007)	A39
χ_P	Slope of linear relationship between V_{pmax} per leaf are at 25°C and N[B,D]	µmol CO_2 $mmol^{-1}$ N s^{-1}	1.1 (sorghum) (Massad *et al.* 2007)	A40
V_{cmax}	Maximum rate of Rubisco carboxylation[F]	µmol CO_2 m^{-2} ground s^{-1}	Table 2	
J_{max}	Maximum rate of electron transport[F]	µmol CO_2 m^{-2} ground s^{-1}	Table 2	
R_d	Leaf day respiration[F]	µmol CO_2 m^{-2} ground s^{-1}	Table 2	
R_m	Mesophyll mitochondrial respiration[D,F]	µmol CO_2 m^{-2} ground s^{-1}	$0.5R_d$ (von Caemmerer 2000)	

(*continued next page*)

Table 1. *(continued)*

Symbol	Description	Units	Value and reference	Equation
K_c	Michaelis-Menten constant of Rubisco for CO_2[F]	µbar	Table 2	
K_o	Michaelis-Menten constant of Rubisco for O_2[F]	µbar	Table 2	
A_c	RuBP-saturated (or Rubisco-limited) net CO_2 assimilation rate[F]	µmol m^{-2} ground s^{-1}	–	
A_j	RuBP-regeneration-limited (or electron-transport-limited) net CO_2 assimilation rate[F]	µmol m^{-2} ground s^{-1}	–	
Γ_*	CO_2 compensation point in the absence of R_d[F]	µbar	–	A52
γ_*	Half the reciprocal of $S_{c/o}$[F]		$0.5/S_{c/o}$	
$S_{c/o}$	Relative CO_2/O_2 specificity of Rubisco[F]	bar bar^{-1}	–	A53
V_{cmax}/V_{omax}	Ratio of maximum rate of Rubisco carboxylation to maximum rate of Rubisco oxygenation[F]		Table 2	A53
J	Potential electron transport rate[F]	µmol e^- m^{-2} ground s^{-1}	–	A46
θ	Empirical curvature factor[A]		0.7 (de Pury and Farquhar 1997)	A46
f	Spectral correction factor[A]		0.15 (de Pury and Farquhar 1997)	A46
I_2	PAR absorbed by PSII[F]	µmol PAR m^{-2} ground s^{-1}	–	A45
α	Fraction of PSII activity in the bundle sheath[A,D]		0.1 (Yin and Struik 2009)	A56
V_p	Rate of PEP carboxylation[D,F]	µmol CO_2 m^{-2} ground s^{-1}	–	A58
V_{pmax}	Maximum PEP carboxylase activity[D,F]	µmol CO_2 m^{-2} ground s^{-1}	Table 2	
K_p	Michaelis-Menten constant of PEP carboxylase for CO_2[D,F]	µbar	Table 2	
$V_{pr,l}$	PEP regeneration rate per leaf area[A,D]	µmol CO_2 m^{-2} leaf s^{-1}	80 (von Caemmerer 2000)	
V_{pr}	PEP regeneration rate[D,F]	µmol CO_2 m^{-2} ground s^{-1}	–	A58
J_t	Potential electron transport rate (symbol for C_4)[D,F]	µmol e^- m^{-2} ground s^{-1}	–	A46
x	Fraction of electron transport partitioned to mesophyll chloroplasts[A,D]		0.4 (von Caemmerer 2000)	A59
		CO_2 diffusion parameters		
C_i	Intercellular airspace CO_2 partial pressure[F]	µbar	–	
C_m	Mesophyll CO_2 partial pressure[D,F]	µbar	–	A57, A60
C_c	Chloroplastic CO_2 partial pressure at the site of Rubisco carboxylation[F]	µbar	–	A51, A54
C_s	Bundle-sheath CO_2 partial pressure[D,F]	µbar	–	A55, A59
O_l	O_2 partial pressure inside C_3 and C_4 leaves[F]	µbar	O_a	
O_c	Chloroplastic O_2 partial pressure at the site of Rubisco carboxylation[F]	µbar	O_l	
O_m	Mesophyll O_2 partial pressure[D,F]	µbar	O_l	A56
O_s	Bundle-sheath O_2 partial pressure[D,F]	µbar	–	A56
a	Slope of linear relationship between C_i/C_a and VPD_a[A]	kPa^{-1}	–0.12 (C_3), –0.19 (C_4) (Zhang and Nobel 1996)	3
b	Intercept of linear relationship between C_i/C_a and VPD_a[A]		0.9 (C_3), 0.84 (C_4) (Zhang and Nobel 1996)	3
C_i/C_a	Ratio of C_i to C_a[F]		–	3
g_m	Mesophyll conductance for CO_2[B,F]	mol CO_2 m^{-2} ground s^{-1} bar^{-1}	Table 2	A47
$g_{bs,l}$	Bundle-sheath conductance for CO_2 per leaf area[A,D]	mol CO_2 m^{-2} leaf s^{-1} bar^{-1}	0.003 (von Caemmerer 2000)	A56

[A]DCaPS input parameters that could be assigned a priori.
[B]DCaPS input parameters that require calibration for different crop species.
[C]Connector with crop models.
[D]Parameters specific to the C_4 photosynthesis model.
[E]DCaPS output to crop models.
[F]Symbol is a calculated variable.

Table 2. C_3 and C_4 temperature response parameters used in Eqns 1 and 2
Note: values marked with 'A' were variable (see Table 1); n.a., not applicable

Parameter	Units	C_3			C_4		
		P_{25}	c (dimensionless)	b (K)	P_{25}	c (dimensionless)	b (K)
K_c	µbar	272.4[A]	32.7[A]	9741.4[A]	1210[D]	25.9[D]	7721.9[D]
K_o	µbar	165800[A]	9.6[A]	2853.0[A]	292000[D]	4.2[D]	1262.9[D]
V_{cmax}/V_{omax}	n.a.	4.6[A]	13.2[A]	3945.7[A]	5.4[D]	9.1[D]	2719.5[D]
V_{cmax}	µmol m^{-2} s^{-1}	A	26.4[B]	7857.8[B]	A	31.5[D]	9381.8[D]
R_d[E]	µmol m^{-2} s^{-1}	A	18.7[B]	5579.7[B]	n.a.	n.a.	n.a.
K_p[F]	µbar	n.a.	n.a.	n.a.	139	14.6[D]	4366.1[D]
V_{pmax}[F]	µmol m^{-2} s^{-1}	n.a.	n.a.	n.a.	A	38.2[D]	11402.4[D]
		P_{25}	T_{opt} (°C)	Ω (K)	P_{25}	T_{opt} (°C)	Ω (K)
J_{max}	µmol m^{-2} s^{-1}	A	28.8[C]	15.5[C]	A	32.6[E]	15.3[E]
g_m	µmol m^{-2} s^{-1} bar^{-1}	0.55	34.3[A]	20.8[A]	0.55	34.3[A]	20.8[A]

[A]Bernacchi *et al.* (2002).
[B]Bernacchi *et al.* (2001).
[C]Farquhar *et al.* (1980).
[D]Boyd *et al.* (2015).
[D]Massad *et al.* (2007).
[E]R_d is assume = 0 in the C_4 model (Massad *et al* 2007).
[F]Parameters specific to the C_4 photosynthesis model.

was calculated by multiplying S_o and the atmospheric transmission ratio (RATIO) (Eqn A4). S_g was then distributed sinusoidally over the diurnal period to derive instantaneous values for incident radiation (I_o MJ m^{-2} ground s^{-1}) (Eqn A3). I_o consists of direct (I_{dir}, MJ m^{-2} ground s^{-1}) and diffuse (I_{dif}, MJ m^{-2} ground s^{-1}) radiation components. Diffuse radiation represents 17% of solar insolation (S_o) for any *Lat*, *DAY* and *RATIO* (Eqn A1). The diurnal pattern of atmospheric transmission of I_{dir} is more complex, so was simply obtained by the difference between I_o and I_{dif} (Eqn A2). This approach allows the proportion of I_{dir} and I_{dif} to vary across a diurnal period giving, for example, higher proportion of I_{dif} in early and later hours of the diurnal period and higher proportion of I_{dif} if *RATIO* is low due to cloud cover.

The derived I_{dir} and I_{dif} (total incident solar radiation) from above were used to estimate direct and diffuse PAR (I_{dir_PAR} and I_{dif_PAR} respectively). It was assumed that 50% of the energy in I_{dir} and I_{dif} was PAR, which was converted to photosynthetic photon flux density by multiplying by 4.56 and 4.25 µmol PAR (J PAR)$^{-1}$ respectively (Eqns A21 and A22). Units for I_{dir_PAR} and I_{dif_PAR} are µmol PAR m^{-2} ground s^{-1}.

The PAR absorbed by either sunlit or shade leaves fractions (I_{abs_sun} and I_{abs_sh}, both with units of µmol PAR m^{-2} s^{-1}) was calculated using the equations of de Pury and Farquhar (1997). This incorporated I_{dir_PAR} and I_{dif_PAR}, optical properties of leaves, such as reflectance and transmittance to PAR, LAI_{can}, and the proportion of intercepted radiation (dependent on canopy-average leaf angle and LAI_{can}). It was assumed that the sunlit leaf fraction received I_{dir_PAR}, I_{dif_PAR} and scattered radiation (caused by reflectance and transmittance of leaves), while the shade leaf fraction received only I_{dif_PAR} and scattered radiation. Detailed equations and calculation procedures are given by Eqns A19–A32 in Appendix 1. In the current model, diurnal variations in leaf reflectance and transmittance are not considered. However, as a first approximation, it can be input into DCaPS for each diurnal simulation.

Air vapour pressure deficit (VPD_a)

Air vapour pressure deficit (VPD_a, kPa) was calculated as the difference between the saturated vapour pressure at air temperature (SVP_a) and that at dew-point temperature (SVP_d) (Eqns A16–A18). The minimum temperature ($T_{a,min}$; more below) for the day was assumed as the dew-point temperature, which has been shown to give robust estimates of VPD_a (Lobell *et al.* 2015). Accordingly, VPD_a varies diurnally with air temperature.

Specific leaf nitrogen (SLN) and photosynthetic physiology

Specific leaf nitrogen (SLN, g N m^{-2} leaf) influences key photosynthetic physiological parameters. Using the mathematical development by de Pury and Farquhar (1997), vertical variation through the canopy can be explicitly incorporated; the approach integrates the profile to give a total for the single-layer canopy, which is then partitioned into sunlit and shade leaves. Distribution of SLN in the canopy was assumed to follow an exponential decay with canopy depth (Eqn A34). The decay function was specified by SLN at the top layer of the canopy (SLN_o, g N m^{-2} leaf) and the average SLN for the canopy (SLN_{av}, g N m^{-2} leaf). To incorporate the effects of SLN on photosynthetic physiology, this model assumed that at the reference temperature of 25°C, the maximum rate of Rubisco carboxylation (V_{cmax}), the maximum rate of electron transport (J_{max}), leaf day respiration (R_d), and the maximum PEP carboxylase activity (V_{pmax}) were all zero below a minimum SLN and increased linearly with slope of χ_V, χ_J, χ_R and χ_P, respectively, above that threshold value (Eqns A37–A40). The minimum SLN values were 0.35 and 0.2 g N m^{-2} (leaf) for C_3 and C_4 respectively (Table 1).

Leaf temperature (T_l)

Estimation of air temperature (T_a, °C) is needed as it significantly influences leaf temperature (T_l, °C). A model of daily T_a (over the 24 h) was used (Eqn A15). Even though the majority of daylight hours can be modelled by the diurnal function of the model, the night time function is sometimes applicable for the early hours of the diurnal period. The diurnal period was modelled with a sine function and an exponential decay function was used during the night. The amplitude of the daily T_a fluctuation was specified by the maximum ($T_{a,max}$, °C) and minimum ($T_{a,min}$, °C) air temperature of the day. The phase shift of the sine function was determined by the lag coefficient for the maximum temperature (x_{lag}), the night-time temperature coefficient (y_{lag}), and the lag of minimum temperature from the time of sunrise (z_{lag}) (Eqn A15). It was assumed here that T_l is approximated by T_a for both sunlit and shade leaf fractions. This is a reasonable assumption over a wide range of temperature under well watered conditions.

The response of photosynthesis to T_l was modelled through responses of the C_3 and C_4 photosynthesis model parameters to T_l (i.e. K_c, K_o, V_{omax}/V_{cmax}, V_{cmax}, J_{max} and R_d for C_3 plus K_p and V_{pmax} for C_4; Table 1). There is a growing availability of these temperature responses, in particular, for model species. The most comprehensive dataset for the C_3 *Nicotiana tabacum* L. have been used effectively for simulating temperature responses of leaf photosynthesis (Bernacchi *et al*. 2002). Temperature responses of K_c, K_o and V_{omax}/V_{cmax} are usually assumed to be similar among C_3 species (von Caemmerer 2013), so here we used parameters from *N. tabacum* for C_3 crop species. It was reported that K_c of *Triticum aestivum* L. is significantly different to *N. tabacum* (Sharwood *et al*. 2016), but whether or not this has significant implications for diurnal canopy photosynthesis will require sensitivity analysis when other wheat parameters also become available. Parameter availability for C_4 crop species is not as comprehensive so here we used parameters for the C_4 model species *Setaria viridis* (L.) P.Beauv. (Boyd *et al*. 2015). These default values can be readily changed as parameters of C_4 crop species become better known.

Temperature responses of K_c, K_o, V_{cmax}, R_d, K_p and V_{pmax} were modelled using an exponential type function (Eqn 1, adapted from Sharkey *et al*. (2007)), whereas J_{max}, due to its apparent optimum in temperature response (Farquhar *et al*. 1980), was modelled via a normal distribution function (Eqn 2, adapted from June *et al*. (2004)). V_{cmax}/V_{omax} and its temperature response were not available from Bernacchi *et al*. (2002), where K_c and K_o were reported, but can be back calculated from K_c, K_o and Γ_* with Eqns A52 and A53 (assuming a chloroplastic oxygen partial pressure (O_c) of 210000 µbar). Its temperature response can be modelled with Eqn 1. In summary, temperature responses of the C_3 and C_4 photosynthesis model parameters to T_l were modelled with Eqn 1 or 2 with parameter values given in Table 2.

Expression of the exponential type function used to describe temperature response of certain photosynthesis model parameters (adapted from Sharkey *et al*. (2007)):

$$P = P_{25}e^{(c-b/(T_l+273))}, \tag{1}$$

where P_{25} is the modelled value of parameter at 25°C, *c* and *b* are empirical constants, which are balanced to give the factor after P_{25} unity at 25°C. Expression of the normal distribution function (adapted from June *et al*. (2004)):

$$P = P_{25}e^{-\left(\frac{T_l-T_{opt}}{\Omega}\right)^2+\left(\frac{25-T_{opt}}{\Omega}\right)^2}, \tag{2}$$

where T_{opt} is the optimum temperature and Ω is the difference in temperature from T_{opt} at which *P* falls to e^{-1} (0.37).

Chloroplastic CO_2 partial pressure (C_c)

Air CO_2 (C_a, µbar) has to diffuse into leaves to reach the carboxylating site of Rubisco inside the chloroplasts for photosynthesis. The best practice for expressing CO_2 levels is in partial pressure (Sharkey *et al*. 2007). To convert from the usual unit of ppm to µbar, it was multiplied by the air pressure (e.g. at sea level, CO_2 of 400 ppm is ($400 \times 10^{-6} \times 1013\,250$ µbar = 405.3 µbar). Leaf boundary-layer and stomatal conductance have significant effects on the drawdown of intercellular airspace CO_2 partial pressure (C_i) relative to C_a (Leuning 1995) and mesophyll conductance has significant effects on the drawdown of CO_2 partial pressure at the carboxylating site of Rubisco (C_c) relative to C_i (Flexas *et al*. 2012). Diffusional conductance, the reciprocal of resistance, of these three components (i.e. leaf boundary-layer (g_{lb}), stomatal (g_s) and mesophyll (g_m) conductance) are incorporated in C_c estimation (Eqn A47) based on Fick's first law of diffusion. To model crop canopies, the turbulent resistance through the canopy boundary layer, which would affect CO_2 partial pressure, air temperature and vapour pressure deficit (relative to those above the canopy), needs to be considered (Leuning *et al*. 1995). However, in their modelling work, Leuning *et al*. (1995) showed simulated canopy photosynthesis reproduced features in data so the omission of the turbulent resistance is a reasonable approximation.

However, there are uncertainties in the estimation of g_{lb} and g_s. The model that is commonly used for g_{lb} estimation relies on leaf width and local wind speed (Goudriaan and van Laar 1994), which cannot be assigned *a priori*. Numerous types of leaf stomatal conductance (g_s) models have been developed over the years (Damour *et al*. 2010). Two particular types are widely used. These are the empirical multiplicative models of environmental influences such as light, C_a and VPD_a (e.g. the Jarvis model; Jarvis (1976)) and the semi-empirical models relating g_s to photosynthesis with VPD_a (e.g. the BWB model (abbreviated using authors' names); Ball *et al*. (1987)), whereas more mechanistic models with plant physiology considerations based on abscisic acid or hydraulic control have also been developed (Damour *et al*. 2010). The limitation of the multiplicative type models is the lack of interactions between plant physiology and among the environmental factors; while the models relating g_s to photosynthesis rely on empirical parameters, which cannot be assigned *a priori*. These empirical coefficients can vary greatly between C_3 species (Li *et al*. 2012) and so cannot be generalised for C_3 crop species, whereas the coefficients are rarely reported for C_4 crop species. Given that there are limited data available to calibrate the empirical coefficients of the Jarvis or the BWB models for C_3 and especially C_4 crop species, an alternative approach to estimate C_i is to use the ratio of C_i/C_a, which is based on stomatal optimisation theory in that stomata respond to maintain a constant C_i under a given C_a to maximise CO_2 assimilation. This ratio (~0.7 for C_3 and ~0.4 for C_4) has been found to be stable with C_a between 100 µbar and 400 µbar in combination with any PPFD between 250 µmol m^{-2} s^{-1} and 2000 µmol m^{-2} s^{-1} (Wong *et al.* 1979); further, C_i/C_a does not appear to change under elevated C_a (Ainsworth and Long 2005). The consistency in C_i/C_a in a wide range of conditions makes it an efficient and robust modelling approach. It is not clear how C_i/C_a would respond to PPFD lower than 250 µmol m^{-2} s^{-1}, but such conditions only apply to the very early and late hours in a diurnal period, which amount to less than ~5% of diurnal canopy photosynthesis and so any changes under such conditions would have limited effect on diurnal total estimation. However, like g_s, C_i/C_a is influenced by VPD_a. It was found to decrease linearly with VPD_a in various species including C_3 *Oryza sativa* and C_4 *Zea mays* (Zhang and Nobel 1996). C_i/C_a response to VPD_a can be given by:

$$C_i/C_a = aVPD_a + b, \qquad (3)$$

where *a* and *b* are empirical constants. For C_3 they are –0.12 and 0.90, respectively; for C_4, they are –0.19 and 0.84 respectively. At VPD_a between 1 to 2 kPa, Eqn 3 gives ~0.7 and 0.5 for C_3 and C_4, respectively, which are similar to those reported by Wong *et al.* (1979). Here, we used the simpler C_i/C_a ratio approach for C_c estimation (Eqn A49), which avoided the need for g_{lb} and g_s.

The importance of mesophyll conductance (g_m) has been recognised only recently. g_m in model C_3 species is known to vary with temperature and there is evidence that g_m may also respond to the other key environmental factors (e.g. irradiance and CO_2), but this variation is not yet completely certain (Pons *et al.* 2009). So here we included only the effect of temperature and modelled this by using the normal distribution function (Eqn 2). At the reference temperature (i.e. 25°C) g_m (per leaf area) in C_3 wheat is assumed to be 0.55 mol CO_2 m^{-2} s^{-1} bar^{-1}. No values for C_4 species have been reported, so the C_3 value was used as a default value.

Diurnal canopy photosynthesis, daily respiration, root and canopy biomass accumulation, and RUE

Diurnal canopy CO_2 assimilation, daily respiration and conversion losses, and allowance for root biomass were used to calculate daily aboveground canopy (shoot) biomass increment ($BIO_{shoot,DAY}$). This model assumes that photosynthesis during the diurnal period results in carbon assimilation for the entire day so we use the symbol $A_{can,DAY}$. $A_{can,DAY}$ was calculated by summing the CO2 assimilation of the sunlit (A_{sun}) and shaded (A_{sh}) leaf fractions of the canopy at the start of each hour over the diurnal period, integrated hourly and summed over the diurnal period (Eqn A73). Using the C_3 and C_4 photosynthesis models, leaf respiration during the diurnal period can be implicitly accounted for at the leaf level with the parameter R_d (Eqns A51, A54, A55 and A59). However, this lacks consideration of respiration from other plant organs and during the night period. A common approach is to omit the leaf-level R_d (by setting χ_R to zero) and consider respiration at the plant level on a daily basis, which can be accounted for within a conversion ratio (*B*) that combines factors allowing for biochemical conversion of CO_2 to biomass and CO_2 loss due to maintenance respiration (Sinclair and Horie 1989). This approach is consistent with the conservative respiration : photosynthesis ratio approach (Gifford 2003), by which plant respiration is taken as a fraction of total canopy photosynthesis. The conversion ratio, *B*, is 0.41 g biomass (g CO_2)$^{-1}$ for cereal crops such as rice and maize (Sinclair and Horie 1989). Therefore, daily whole-plant biomass increment ($BIO_{total,DAY}$) was calculated by multiplying $A_{can,DAY}$ with the molecular weight of CO_2 (= 44 g (mol CO_2)$^{-1}$) and *B*. To calculate shoot biomass increment ($BIO_{shoot,DAY}$), $BIO_{total,DAY}$ is multiplied by the fraction of aboveground (shoot) biomass to total biomass (shoot + root), denoted by P_{shoot} (Eqn A74). In effect, this simulates partitioning of a fraction of $BIO_{total,DAY}$ to root. Here, P_{shoot} is given a default of 1 assuming a mature canopy around flowering. The RUE for the day (RUE_{DAY}, g biomass MJ^{-1}) was then calculated by dividing $BIO_{shoot,DAY}$ by the total amount of intercepted solar radiation (Eqns A75 and A76 respectively).

Model rationality analysis

Environmental parameters

Default environmental parameters were set for C_3 wheat (winter crop) and C_4 sorghum (summer crop), with a canopy leaf area index (LAI_{can}) = 6, growing in the southern hemisphere spring (DAY = 298) and summer (DAY = 15), respectively, at locations with Lat = –35° and –27.5° respectively. Clear sky with atmospheric transmission ratio (RATIO) of 0.75 was assumed unless otherwise stated. The average maximum and minimum air temperatures at these times of year were 21 and 7°C for Lat = –35° and 30 and 15°C for Lat = –27.5°.

Diurnal canopy photosynthesis in relation to canopy architecture

Diurnal patterns of net C_3 and C_4 canopy photosynthesis for a range of canopy LAI (LAI_{can}) and canopy-average leaf inclination relative to the horizontal (β) were simulated as a qualitative test of the DCaPS. The C_4 simulations (Fig. 2*c, d*) were consistent in the diurnal pattern and magnitude with those reported by Duncan *et al.* (1967) and Hammer *et al.* (2009), who found that the canopy with erect leaves (β = 80°) continued to increase canopy photosynthetic rate beyond LAI_{can} = 4 at high LAI_{can} (= 8) due to better light distribution throughout the canopy. There was ~40% increase in midday canopy photosynthetic rate at LAI_{can} = 8 compared with LAI_{can} = 4, which was comparable to that simulated by Duncan *et al.* (1967) and Hammer *et al.* (2009). In the canopy with less erect leaves (β = 40°), there was little increase in canopy photosynthetic rate with increase in LAI_{can} beyond 4. In terms of the magnitude, the simulated canopy photosynthetic rate at LAI_{can} = 4 (Fig. 2*c, d*) was comparable to that observed in a similar size maize canopy (~70 µmol CO_2 m^{-2} s^{-1}) by Grant *et al.* (1989). The simulation also indicated that for a canopy with low LAI_{can} (= 2), less erect leaves (β = 40°) offered greater PAR absorption by both sunlit and shade leaf fractions consistent with greater radiation interception as found by Hammer *et al.* (2009). Even though the sunlit LAI (LAI_{sun}) can be reduced up to 30% with less erect leaves, its photosynthetic rate was not affected due to associated increase in absorbed PAR. For the case of the shade leaf fraction, the increase in both the absorbed PAR and shade LAI (LAI_{sh}) significantly increased shade leaf $A_{j,sh}$. These consequences for the two leaf fractions translate to a greater canopy photosynthesis

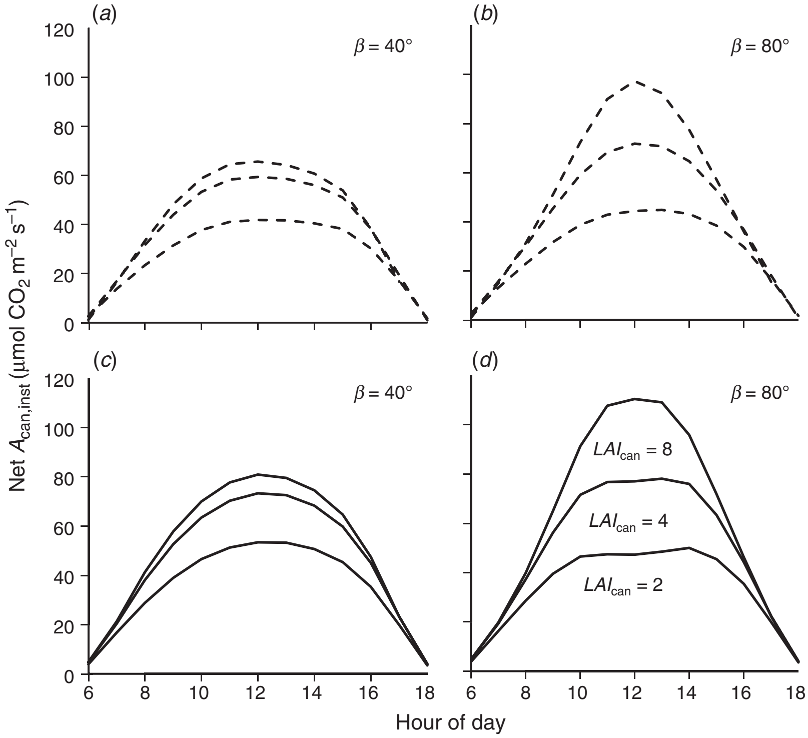

Fig. 2. Diurnal net C_3 (upper panels) and C_4 (lower panels) canopy photosynthesis with various combinations of canopy attributes: leaf area index (LAI_{can}) of 2, 4 or 8 and canopy-average leaf inclination relative to the horizontal (β) of 40° (*a*, *c*) or 80° (*b*, *d*). In all four panels, the lower, middle and top curves show results for LAI_{can} of 2, 4 and 8 respectively. Default values of other model parameters are given in Tables 1, 2.

with less erect leaves at low LAI_{can}. The effects of leaf erectness were mostly analogous for the C_3 simulations (Fig. 2*a, b*). However, the greater radiation interception offered by less erect leaves at low LAI_{can} did not translate to greater canopy photosynthesis. Unlike C_4, reduction in LAI_{sun} significantly reduced the Rubisco-limited photosynthetic rate ($A_{c,sun}$) resulting in reduced photosynthetic rate in the sunlit leaf fraction. This more than offset the increase (because of increase in both the absorbed PAR and LAI_{sh}) in $A_{j,sh}$. So in the case of C_3, Rubisco limitation can reduce photosynthetic rate of small (low LAI_{can}) canopies with less erect leaves.

Diurnal canopy photosynthesis in relation to CO_2 with varying temperature

A simulation of net C_3 and C_4 diurnal canopy photosynthesis ($A_{can,DAY}$) for a range of air CO_2 partial pressures (C_a) and temperatures (T_a) was undertaken as a qualitative test. Based on various large-scale free-air CO_2 enrichment (FACE) studies, elevating C_a to 475–600 μbar (or an average of 540 μbar) increased C_3 $A_{can,DAY}$ by an average of 28% relative to C_a = 360 μbar (Ainsworth and Long 2005). This increase was reproduced when T_{a_min} and T_{a_max} were set to 14 and 28°C, respectively, simulating hot days for winter wheat crops (Fig. 3). Ainsworth and Long (2005) noted that when the large-scale free-air CO_2 enrichment (FACE) studies were categorised by temperature, the relative increase in light saturated photosynthesis was lower (an average of 19%) at lower temperatures (<25°C). Simulation results for average days with T_{a_min} and T_{a_max} of 7 and 21°C, respectively, is consistent with this CO_2 response at lower temperatures (Fig. 3). The increase in $A_{can,DAY}$ can be as high as 50% at C_a = 1000 μbar. This result is discussed further below in regards to daily radiation use efficiency. In the case of C_4 canopy photosynthesis, the response of net $A_{can,DAY}$ to C_a and temperature was significantly less, which is consistent with the finding that C_4 maize photosynthesis is not significantly affected by elevated C_a (Leakey *et al*. 2006). This simulation suggested that canopy photosynthesis of C_3 crops can significantly benefit from elevated CO_2, while C_4 crops do not.

RUE_{DAY} in relation to CO_2 with varying temperature

A simulation of C_3 and C_4 daily canopy radiation use efficiency (RUE_{DAY}) for a range of air CO_2 partial pressures (C_a) and air temperatures (T_a) was also undertaken as a qualitative test. Elevated C_a is known to increase the net photosynthetic rate of C_3 plants resulting in increased biomass accumulation and RUE (Kimball *et al*. 2002) and there is also an enhanced effect on RUE at higher T_a (Reyenga *et al*. 1999). The general consensus is that RUE of C_3 crops increases almost linearly from C_a of 300 to 660 μbar, reaches ~30% increase at double the ambient C_a and plateaus at ~50% beyond C_a of 1000 μbar (Lobell *et al*. 2015). O'Leary *et al*. (2015) found a ~22% increase in wheat crop biomass in response to elevated C_a from 365 to 550 μmol mol^{-1}. These known responses of C_3 RUE were reproduced with the model for winter wheat crops experiencing average to hot

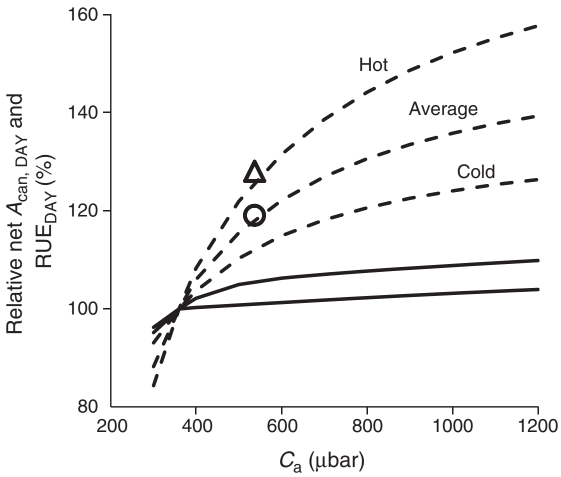

Fig. 3. Relative net C_3 (dashed curves) and C_4 (solid curves) daily canopy photosynthesis ($A_{can,DAY}$) and radiation use efficiency on a daily basis (RUE$_{DAY}$) in response to air CO_2 and temperature. $A_{can,DAY}$ or RUE$_{DAY}$ curves were normalised to their respective values at an air CO_2 partial pressure (C_a) = 360 µbar respectively. Days were categorised as hot (14–28°C), average (7–21°C) or cold (0–14°C) for winter wheat crops; temperatures were not assigned to C_4 curves due to their small response to C_a. The triangle indicates a 28% increase in $A_{can,DAY}$ at an average C_a of 540 µbar on hot days, relative to that at C_a = 360 µbar; the circle indicates a 19% increase in relative $A_{can,DAY}$ increase on average days at the same average C_a. These relative increases were taken from work by Ainsworth and Long (2005). Default values of other model parameters are given in Tables 1, 2.

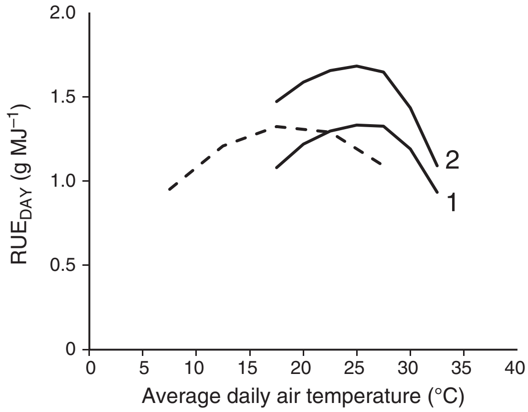

Fig. 4. Radiation use efficiency on a daily basis of C_3 (dashed curve) and C_4 (solid curve) canopy in response to temperature. RUE$_{DAY}$ is plotted against average daily air temperature, which is calculated by averaging the daily maximum ($T_{a,max}$) and minimum ($T_{a,min}$) air temperatures; $T_{a,max} = T_{a,min} + 15$ with $T_{a,min}$ = 0–20°C for C_3 and 10–25°C for C_4. Solid curve 1 was simulated for a dwarf hybrid sorghum with the slope of the linear relationship between the maximum rate of Rubisco carboxylation (χ_{Vc}), maximum rate of electron transport (χ_J), maximum PEP carboxylase activity (χ_{VP}) and specific leaf nitrogen of 0.5, 2.4 and 1.0 µmol CO_2 (mmol N)$^{-1}$ s^{-1}, respectively; solid curve 2 was simulated for maize and tall hybrid sorghum with χ_{Vc}, χ_J and χ_{VP} of 1.0, 4.0 and 2.0 µmol CO_2 (mmol N)$^{-1}$ s^{-1} respectively. Default values of other model parameters are given in Tables 1, 2.

temperatures (Fig. 3). The response relative of RUE$_{DAY}$ to C_a and temperature reflect that of net $A_{can,DAY}$ because of the linear relationship between RUE$_{DAY}$ and $A_{can,DAY}$ (Eqns A74 and A75). In the case of the C_4 canopy, elevated C_a had only a small effect on the simulated RUE$_{DAY}$ (Fig. 3), which was consistent with a lack of response to C_a observed in C_4 sorghum. This simulation suggested that elevated CO_2 can significantly benefit canopy biomass accumulation of C_3 crops, but not C_4 crops.

RUE$_{DAY}$ in relation to average temperature

A simulation of C_3 and C_4 daily canopy radiation use efficiency (RUE$_{DAY}$) for a range of average air temperature was undertaken as a qualitative test. Air temperature (T_a) varies diurnally between the daily maximum ($T_{a,max}$) and minimum ($T_{a,min}$) temperature and the diurnal pattern can be modelled with Eqn A15. A 15°C difference between $T_{a,max}$ and $T_{a,min}$ was assumed and a range of temperature used so that temperatures ranging from 0–35°C for C_3 and 10–40°C for C_4 were included. When plotted against average daily temperature the simulated RUE$_{DAY}$ was relatively insensitive between average temperatures of 14–23°C for C_3 and 21–28°C for C_4 (Fig. 4). This is consistent with known insensitivities of crop biomass accumulation and RUE to temperatures around optimal values (Yan and Hunt 1999). These temperature ranges for C_3 and C_4 responses were associated with the response of leaf photosynthesis to temperature, which is also insensitive within a broad range (e.g. C_3, rice and wheat (Nagai and Makino 2009); C_4, various grasses (Ludlow 1981), maize (response curve was derived from picking a typical C_i (e.g. 150 µbar) in A/C_i curves measured at different temperature in Massad *et al*. (2007)). Further, RUE under optimum growth conditions has been reported as 1.2–1.5 g MJ^{-1} for wheat (Fischer *et al*. 2014) and 1.2–1.4 g MJ^{-1} for dwarf sorghum (George-Jaeggli *et al*. 2013). The simulated maximum RUE$_{DAY}$ for C_3 and C_4 corresponded with these reported ranges (Fig. 4).

The comparison here between C_3 wheat and C_4 dwarf sorghum RUE does not reveal differences in magnitude between C_3 and C_4 crops, where the latter is typically higher. RUE of some tall hybrid sorghum varieties (George-Jaeggli *et al*. 2013) and maize (Sinclair and Muchow 1999) was found to be as high as 1.6–1.8 g MJ^{-1}, or possibly even higher (2.0–2.2 g MJ^{-1}) during the rapid stem elongation and maximum biomass accumulation phase (Olson *et al*. 2012). The typical high C_4 RUE could be ascribed to higher photosynthetic rate (Hammer *et al*. 2010) and/or differences in canopy architecture, which may affect diurnal canopy photosynthesis (Fig. 2). These scenarios (and their combinations) can be simulated with the model. As a demonstration of this capability, we have assumed the first case by increasing the slope of the linear relationship between the maximum rate of Rubisco carboxylation (χ_{Vc}), maximum rate of electron transport (χ_J), maximum PEP carboxylase activity (χ_{VP}) and specific leaf nitrogen; these gave greater V_{cmax}, J_{max} and V_{pmax}, respectively, and simulated the typical high RUE in C_4 crops (Fig. 4).

RUE$_{DAY}$ in relation to SLN$_{av}$ with varying direct : diffuse radiation

A simulation of C_3 and C_4 RUE$_{DAY}$ for a range of canopy-average specific leaf nitrogen (SLN$_{av}$) with varying direct : diffuse radiation was undertaken as a qualitative test. Direct : diffuse radiation was varied by changing the atmospheric transmission ratio (RATIO) in a similar manner to the simulation study by Hammer and Wright (1994). High values (*RATIO* = 0.75) reflect clear sky with high transmission of direct radiation and a low fraction of diffuse radiation. Massignam (2003) found that RUE of the C_3 crop sunflower responded asymptotically to SLN_{av} with RUE of ~1 and 1.5 g MJ^{-1} at SLN_{av} of 1.5 and 2 g N m^{-2} respectively. This was closely predicted by the model with clear sky conditions (Fig. 5*a*). Muchow and Sinclair (1994) found that RUE of field-grown dwarf sorghum responded asymptotically to SLN_{av}, but did not approach the asymptote because sorghum SLN_{av} maximised at 1.3 g N m^{-2} giving RUE of 1.26 g MJ^{-1}. This was also closely predicted by the model with clear sky conditions (Fig. 5*b*). The simulated RUE_{DAY} response of typical dwarf sorghum was not significantly different from that for wheat, but when the model was parameterised for the greater photosynthetic rate of the tall hybrid sorghums, the response was higher at all SLN_{av} (Fig. 5*b*). These responses were comparable to that of maize crops (RUE of ~1.5 and 2 g MJ^{-1} at SLN_{av} of 1 and 2 g N m^{-2} respectively) (Massignam 2003). In general, direct radiation level was higher with higher RATIO, while the absolute level of diffuse radiation was insensitive to RATIO, leading to a greater fraction of diffuse at low RATIO (cloudy days). Simulated results of increasing diffuse radiation fraction on C_3 species (Fig. 5*a*) were consistent with Tubiello *et al*. (1997), who found a significant increase (~40%) in wheat RUE when grown under high diffuse radiation conditions due to the fact that diffuse radiation penetrates deeper into the crop canopy and increases photosynthetic rate of the lower leaves. Hammer and Wright (1994) used a simpler canopy photosynthesis model to show that decreases in RATIO caused RUE to increase. This response of RUE_{DAY} to RATIO was reproduced (Fig. 5). Although both C_3 and C_4 types responded similarly to the increased fraction of diffuse radiation, the standard C_4 types achieved higher RUE_{DAY} at much lower SLN_{av} as a result of their greater photosynthetic rate (Fig. 5*b*). This is consistent with the comparison of responses reported by Sinclair and Horie (1989).

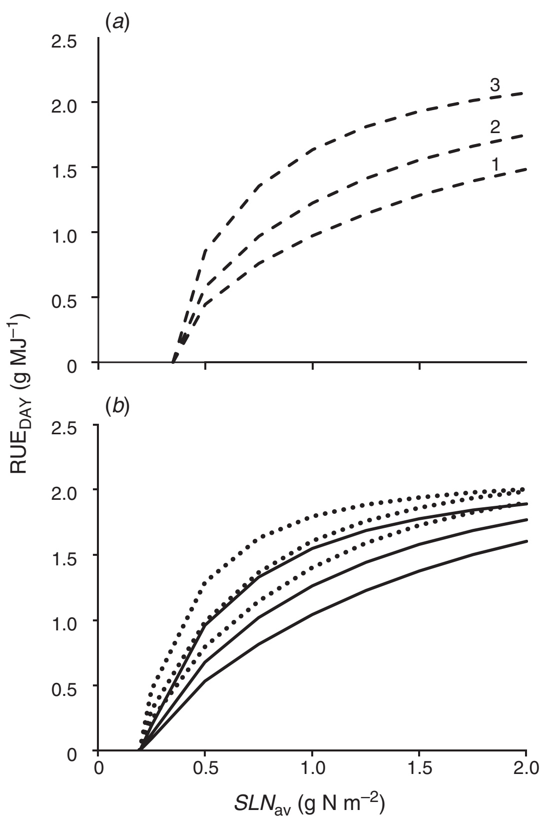

Fig. 5. Radiation use efficiency on a daily basis for (*a*) C_3 and (*b*) C_4 canopy in response to specific leaf nitrogen and solar radiation levels. RUE_{DAY} is plotted against canopy-average specific leaf nitrogen (SLN_{av}). Curves 1 (lowest curve), 2 and 3 (highest curve) are obtained by setting RATIO to 0.75 (clear sky), 0.55 and 0.35 (heavy cloud cover), respectively, which changes the amount of incident radiation (curve 1 greatest) and the proportion that is diffuse (curve 3 greatest). This order applies to (*b*) as well. Dotted curves in panel (*b*) show simulated RUE_{DAY} for a standard C_4 crop (e.g. maize) with χ_V, χ_J and χ_P of 1.0, 4.0 and 2.0 µmol CO_2 (mmol N)$^{-1}$ s^{-1} respectively. Default values of other model parameters are given in Tables 1, 2.

Applications for photosynthesis manipulation – a tool for assessing consequences of photosynthetic changes

The Diurnal Canopy Photosynthesis Simulator (DCaPS) enables simulation of likely canopy-level consequences of photosynthetic manipulation and canopy structural attributes in C_3 and C_4 field crops. It integrates many non-linear responses of leaf photosynthesis to environment and processes involved in upscaling to the canopy level (see 'Model detail').

Considerable effort has been invested to develop DCaPS into an interactive web-based application (www.dcaps.net.au), which can be run with internet browsers on any major platform without prior installation of DCaPS (DCaPS v1.0 source code is available at https://github.com/QAAFI/DCaPS.git, accessed 16 October 2017). This web-based application is conveniently available for experimentalists working on photosynthetic research and/or as a teaching tool. DCaPS can be parameterised for a range of environments, canopy attributes and photosynthetic physiology. The online application reports diurnal patterns of environmental variables, diurnal canopy photosynthesis and daily canopy biomass increment.

Here we present two examples of using DCaPS to simulate consequences of changing photosynthetic attributes in both C_3 and C_4. These are simplified examples to demonstrate the capacity of DCaPS to capture complex dynamic interactions between photosynthetic physiology and diurnal variations in environment, which are not mechanistically included in, for example, the RUE type of canopy photosynthesis models. Users need to be aware of possible concomitant changes associated with changing model parameters. However, knowledge generated from exercising this model could inform photosynthetic manipulation efforts for assisting field crop improvement.

Relative CO_2/O_2 specificity of Rubisco

Increasing the relative CO_2/O_2 specificity of Rubisco ($S_{c/o}$) is a strategy for increasing CO_2 assimilation in isolated leaves (Evans 2013). There are likely concomitant changes associated with changing $S_{c/o}$ (Evans 2013). However, in this simulation, we have minimised complexity by assuming all other parameters are kept at default values (Tables 1, 2).

Using DCaPS, it was estimated that a significant (25%) increase in $S_{c/o}$, could increase C_3 and C_4 diurnal canopy photosynthetic rate ($A_{can,DAY}$) by ~6.0% and 2.5%, respectively, assuming all other parameters were kept at default values (Tables 1, 2). When $S_{c/o}$ was set to increase by 25%, much of the enhancement was not translated to increase in photosynthetic rate as Rubisco-limited photosynthesis is less sensitive to changes in $S_{c/o}$ than electron transport limited photosynthesis. In addition, differential effects on sunlit and shaded leaves associated with the canopy light environment contributed to this overall outcome when integrated to the canopy level. Fig. 6*a–f* shows the changes to instantaneous photosynthesis of the sunlit and shade leaf fractions throughout the day.

In the case of C_3, Rubisco-limited ($A_{c,sun}$) and electron-transport-limited ($A_{j,sun}$) photosynthetic rates of the sunlit leaf fraction increased by an average of 2.6 and 7.2% over the diurnal cycle, respectively (Fig. 6*b*). However, between 11 : 00 and 15 : 00 hours, when the canopy had a high photosynthetic rate, the sunlit leaf fraction was Rubisco ($A_{c,sun}$) limited. This interplay between A_c and A_j limitation throughout the day resulted in only 5.5% increase as opposed to the potential 7.2%. On the other hand, the shade leaf fraction increased by 7.7% over the diurnal cycle (all contributed by effects on electron-transport-limited rate (A_j)) (Fig. 6*c*). Altogether, compared with a potential 7.2% increase in $A_{can,DAY}$, A_c limitation around noon reduced the potential increase in $A_{can,DAY}$ to 6.0%.

C_4 canopy photosynthesis was less responsive to changes in $S_{c/o}$ than C_3, which was consistent with the notion that increasing $S_{c/o}$ in C_4 plants has less effect on photosynthesis as they have evolved CO_2-concentrating mechanisms for enhanced photosynthesis. In the case of C_4 canopy photosynthesis, there was no interplay between Rubisco and electron transport limitations with all effects related to the latter (i.e. A_j) (Fig. 6*e, f*), and totalling to a 2.5% increase in $A_{can,DAY}$.

Rubisco activity and electron-transport rate

There is evidence that Rubisco activity and electron transport capacity can vary among species, can respond to the prevailing environment, and be bioengineered (reviewed by Evans (2013)). Putative changes in Rubisco activity and electron transport capacity can be implemented in the C_3 and C_4 photosynthesis models of DCaPS through changing the slope of the linear relationship between the maximum rate of Rubisco carboxylation (χ_{Vc}), the maximum rate of electron transport (χ_J) and specific leaf nitrogen; giving greater V_{cmax} and J_{max}, respectively. Here we examine diurnal canopy photosynthesis consequences of such variations.

The simulation of consequences on diurnal canopy photosynthesis of changes in V_{cmax} and J_{max} for C_3 and C_4 types are presented in Fig. 6*g–n*. $A_{can,DAY}$ did not respond to increase in V_{cmax} for C_3 types because both the sunlit and shade leaf fractions were mostly electron transport (A_j) limited in the reference scenario (Fig. 6*g*) and any increase in Rubisco activity (A_c) was not useful (Fig. 6*h*). However, increasing J_{max} could increase $A_{can,DAY}$ by 4.5%, which was attributed to higher electron-transport limited photosynthetic rate of the sunlit leaf fraction ($A_{j,sun}$) during early and late hours of the day (Fig. 6*i*). The largest effect was when V_{cmax} and J_{max} were both increased by 20%, which gave a 9.5% increase in $A_{can,DAY}$. This shifted the whole diurnal photosynthetic rate higher (Fig. 6*j*). It was apparent that the sunlit fraction of the canopy was more sensitive to these changes and contributed most to the higher canopy photosynthesis.

For C_4 canopy photosynthesis, there was less interplay between Rubisco- and electron-transport-limited photosynthetic rate. C_4 canopy photosynthesis was always electron-transport limited (Fig. 6*k*). Hence, increase in Rubisco activity (V_{cmax}) had little or no effect on $A_{can,DAY}$ (Fig. 6*l*). However, a 20% increase in maximum rate of electron transport (J_{max}) increased $A_{can,DAY}$ significantly (6%) (Fig. 6*m*) and increasing both J_{max} and V_{cmax} simultaneously, increased $A_{can,DAY}$ by 8% (Fig. 6*n*).

Implications for crop performance prediction – connecting biochemical photosynthesis models with crop models for seasonal simulations

Many crop models incorporate canopy photosynthesis as a key driver for crop growth for seasonal simulation. In some of these models, under well watered conditions, canopy CO_2 assimilation/biomass accumulation is based on the empirical RUE approach, while others incorporate more detailed models of photosynthetic light response (PLR). Depending on the detail required for canopy photosynthesis simulation, either type of model can be used. However, the intrinsic empirical nature of these approaches makes it difficult to realistically model responses to manipulation of photosynthetic processes and environmental effects and so that often simple empirical indices are invoked to generate possible effects (Wu *et al*. 2016).

In this study, we have shown that the DCaPS can rationally simulate canopy photosynthetic rate responses to photosynthetic physiology, key environmental factors and crop status (e.g. light, C_a, T_a and SLN_{av}). This provides confidence in incorporating DCaPS into crop growth and development models to drive aboveground canopy biomass accumulation in seasonal simulations. The capacity to connect with photosynthetic attributes makes DCaPS a valuable tool to improve the biological functionality of crop models in terms of aboveground canopy biomass accumulation under well watered conditions.

At first inspection, it may seem unduly complicated to introduce DCaPS into a crop model due to the parameterisation requirements at the biochemical/leaf level (Table 1). However, many are related to a small subset of key parameters, while others (e.g. temperature response parameters, Table 2) can be assigned *a priori* depending on the application of DCaPS. For example, the parameter values for kinetic properties of Rubisco (i.e. K_c, K_o, V_{cmax}/V_{omax}) and their temperature responses are relatively conserved within C_3 species (von Caemmerer 2013). This means parameter values obtained from extensively studied model species, such as *Arabidopsis* and tobacco, can be used for C_3 crop species. Further, more comprehensive parameter values for C_3 (Braune *et al*. 2009) and C_4 (von Caemmerer 2000; Massad *et al*. 2007) crop species are also emerging. This leaves a small set of parameters (three and four parameters for C_3 and C_4 respectively) to be assigned as indicated in Table 1.

To facilitate connection with crop growth and development simulation models, DCaPS, which operates on a daily timescale,

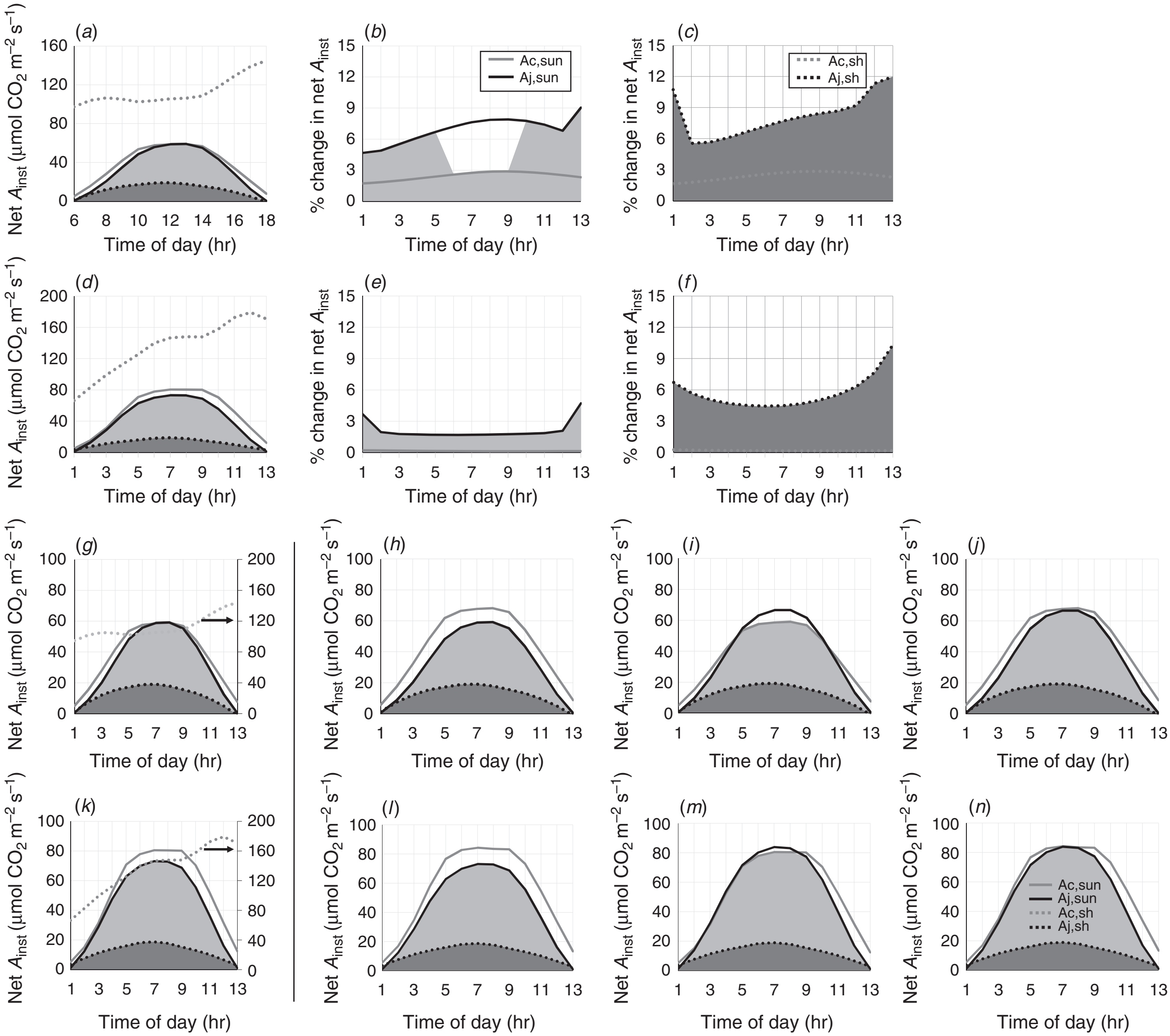

Fig. 6. Dirunal C_3 and C_4 canopy photosynthesis and photosynthetic changes. The top two rows (C_3 and C_4 respectively) show % changes in diurnal canopy photosynthesis with 25% increase in the relative CO_2/O_2 specificity of Rubisco ($S_{c/o}$). (*a*, *d*) Reference net A_{inst} at default $S_{c/o}$; (*b*, *e*) % changes in net A_{inst} for the sunlit leaf fraction of the canopy; (*c*, *f*) % changes in net A_{inst} for the shade leaf fraction. The bottom two rows (C_3 and C_4 respectively) show changes in diurnal canopy photosynthesis with various Rubisco activity (V_{cmax}) and/or electron transport capacity (J_{max}). (*g*, *k*) Reference net A_{inst} with default values; (*h*, *l*) V_{cmax} increased by 20%; (*i*, *m*) J_{max} increased by 20%; (*j*, *n*) V_{cmax} and J_{max} both increased by 20%. Solid and dotted curves show values for the sunlit (A_{sun}) and shade (A_{sh}) leaf fractions of the canopy, respectively; grey and black colour coding are for Rubisco-limited (A_c) and electron-transport limited (A_j) photosynthetic rate, respectively. The $A_{c,sh}$ curve is removed from *h*, *i*, *j*, *l*, *m* and *n* except in *g* and *k* where it is plotted using the right hand ordinate (indicated by arrows). Light grey areas indicate CO_2 assimilation rate or its % change in the sunlit leaf fraction and dark grey areas indicate the same for the shade leaf fraction. For each leaf fraction, photosynthetic rate is given by the minimum of A_c and A_j. Note that diurnal canopy photosynthesis ($A_{can,DAY}$; see text) is obtained by summing the photosynthetic rate of the two leaf fractions, integrate hourly and sum over the diurnal period. Default values of other model parameters are given in Tables 1 and 2.

needs to be connected with environmental and crop canopy attribute data that vary throughout the growing season. These data, already used and output by some crop models, can be input on a daily frequency into DCaPS at the start of each daily simulation. Recall that DCaPS incorporates four key environmental parameters (radiation, T_a, VPD_a, C_a) and the three parameters for canopy attributes (LAI_{can}, β (canopy-average leaf inclination relative to the horizontal) and SLN_{av}). Radiation, T_a, VPD_a, LAI_{can} and SLN_{av} can be connected with daily values supplied by crop models such as APSIM (Hammer *et al.* 2009, 2010). This leaves C_a and β to be assigned. It would be reasonable to assume C_a as a constant, while β can be reasonably estimated if a spherical leaf-angle distribution is assumed for field crops (Eqn A26). The design of DCaPS, which accepts daily values of environmental parameters and crop attributes allows convenient connection with crop models for seasonal simulation.

Conflicts of interest

The authors declare no conflicts of interest.

Acknowledgements

The work is financially supported by the ARC Centre of Excellence for Translational Photosynthesis, funded by the Australian Research Council's Centre of Excellence funding program. The authors acknowledge helpful discussions with Dr Erik van Oosterom in relation to the model schematic, Professor John Evans and Professor Susanne von Caemmerer in relation to the C_3 and C_4 photosynthesis models as well as providing useful references, Dr Enli Wang in relation to temperature response of leaf photosynthesis as well as providing useful references, and the National eResearch Collaboration Tools and Resources (NECTAR) for providing a free web server for hosting dcaps.net.au.

References

Ainsworth EA, Long SP (2005) What have we learned from 15 years of free-air CO2 enrichment (FACE)? A meta-analytic review of the responses of photosynthesis, canopy properties and plant production to rising CO_2. *New Phytologist* **165**, 351–372. doi:10.1111/j.1469-8137.2004.01224.x

Ball JT, Woodrow I, Berry J (1987) A model predicting stomatal conductance and its contribution to the control of photosynthesis under different environmental conditions. In 'Progress in photosynthesis research'. (Ed. J Biggins) pp. 221–224. (Martinus Nijhoff Publishers: Dordrecht, The Netherlands)

Bernacchi CJ, Singsaas EL, Pimentel C, Portis AR Jr, Long SP (2001) Improved temperature response functions for models of Rubisco-limited photosynthesis. *Plant, Cell & Environment* **24**, 253–259. doi:10.1111/j.1365-3040.2001.00668.x

Bernacchi CJ, Portis AR, Nakano H, von Caemmerer S, Long SP (2002) Temperature response of mesophyll conductance. Implications for the determination of Rubisco enzyme kinetics and for limitations to photosynthesis *in vivo*. *Plant Physiology* **130**, 1992–1998. doi:10.1104/pp.008250

Boyd RA, Gandin A, Cousins AB (2015) Temperature response of C_4 photosynthesis: biochemical analysis of Rubisco, phospho*enol*pyruvate carboxylase and carbonic anhydrase in *Setaria viridis*. *Plant Physiology* **169**, 1850–1861.

Braune H, Mueller J, Diepenbrock W (2009) Integrating effects of leaf nitrogen, age, rank, and growth temperature into the photosynthesis-stomatal conductance model LEAFC3-N parameterised for barley (*Hordeum vulgare* L.). *Ecological Modelling* **220**, 1599–1612. doi:10.1016/j.ecolmodel.2009.03.027

Damour G, Simonneau T, Cochard H, Urban L (2010) An overview of models of stomatal conductance at the leaf level. *Plant, Cell & Environment* **33**, 1419–1438.

de Pury DGG, Farquhar GD (1997) Simple scaling of photosynthesis from leaves to canopies without the errors of big-leaf models. *Plant, Cell & Environment* **20**, 537–557. doi:10.1111/j.1365-3040.1997.00094.x

Duncan WG, Loomis RS, Williams WA, Hanau R (1967) A model for simulating photosynthesis in plant communities. *Hilgardia* **38**, 181–205. doi:10.3733/hilg.v38n04p181

Evans JR (2013) Improving photosynthesis. *Plant Physiology* **162**, 1780–1793. doi:10.1104/pp.113.219006

Farquhar GD, von Caemmerer S, Berry JA (1980) A biochemical model of photosynthetic CO_2 assimilation in leaves of C_3 species. *Planta* **149**, 78–90. doi:10.1007/BF00386231

Fischer T, Byerlee D, Greg E (2014) Crop yields and global food security: will yield increase continue to feed the world? ACIAR Monograph 158. Australian Centre for International Agricultural Research, Canberra, Australia.

Flexas J, Barbour MM, Brendel O, Cabrera HM, Carriqui M, Diaz-Espejo A, Douthe C, Dreyer E, Ferrio JP, Gago J, Galle A, Galmes J, Kodama N, Medrano H, Niinemets U, Peguero-Pina JJ, Pou A, Ribas-Carbo M, Tomas M, Tosens T, Warren CR (2012) Mesophyll diffusion conductance to CO_2: an unappreciated central player in photosynthesis. *Plant Science* **193–194**, 70–84. doi:10.1016/j.plantsci.2012.05.009

George-Jaeggli B, Jordan DR, van Oosterom EJ, Broad IJ, Hammer GL (2013) Sorghum dwarfing genes can affect radiation capture and radiation use efficiency. *Field Crops Research* **149**, 283–290. doi:10.1016/j.fcr.2013.05.005

Gifford RM (2003) Plant respiration in productivity models: conceptualisation, representation and issues for global terrestrial carbon-cycle research. *Functional Plant Biology* **30**, 171–186. doi:10.1071/FP02083

Goudriaan J, van Laar HH (1994) 'Modelling potential crop growth processes: textbook with exercises.' (Kluwer Academic Publishers: Dordrecht, The Netherlands)

Grant RF, Peters DB, Larson EM, Huck MG (1989) Simulation of canopy photosynthesis in maize and soybean. *Agricultural and Forest Meteorology* **48**, 75–92. doi:10.1016/0168-1923(89)90008-7

Hammer GL, Wright GC (1994) A theoretical-analysis of nitrogen and radiation effects on radiation use efficiency in peanut. *Australian Journal of Agricultural Research* **45**, 575–589. doi:10.1071/AR9940575

Hammer GL, Dong Z, McLean G, Doherty A, Messina C, Schussler J, Zinselmeier C, Paszkiewicz S, Cooper M (2009) Can changes in canopy and/or root system architecture explain historical maize yield trends in the US corn belt? *Crop Science* **49**, 299–312. doi:10.2135/cropsci2008.03.0152

Hammer GL, van Oosterom E, McLean G, Chapman SC, Broad I, Harland P, Muchow RC (2010) Adapting APSIM to model the physiology and genetics of complex adaptive traits in field crops. *Journal of Experimental Botany* **61**, 2185–2202. doi:10.1093/jxb/erq095

Humphries SW, Long SP (1995) WIMOVAC – a software package for modeling the dynamics of plant leaf and canopy photosynthesis. *Computer Applications in the Biosciences* **11**, 361–371.

Jarvis PG (1976) Interpretation of variations in leaf water potential and stomatal conductance found in canopies in field. *Philosophical Transactions of the Royal Society of London. Series B, Biological Sciences* **273**, 593–610. doi:10.1098/rstb.1976.0035

June T, Evans JR, Farquhar GD (2004) A simple new equation for the reversible temperature dependence of photosynthetic electron transport: a study on soybean leaf. *Functional Plant Biology* **31**, 275–283. doi:10.1071/FP03250

Kimball BA, Kobayashi K, Bindi M (2002) Responses of agricultural crops to free-air CO_2 enrichment. In 'Advances in agronomy. Vol. 77'. (Ed. LS Donald) pp. 293–368. (Academic Press: Cambridge, MA, USA)

Leakey ADB, Uribelarrea M, Ainsworth EA, Naidu SL, Rogers A, Ort DR, Long SP (2006) Photosynthesis, productivity, and yield of maize are not affected by open-air elevation of CO_2 concentration in the absence of drought. *Plant Physiology* **140**, 779–790. doi:10.1104/pp.105.073957

Leuning R (1995) A critical-appraisal of a combined stomatal-photosynthesis model for C_3 plants. *Plant, Cell & Environment* **18**, 339–355. doi:10.1111/j.1365-3040.1995.tb00370.x

Leuning R, Kelliher FM, De Pury DGG, Schulze ED (1995) Leaf nitrogen, photosynthesis, conductance and transpiration: scaling from leaves to canopies. *Plant, Cell & Environment* **18**, 1183–1200. doi:10.1111/j.1365-3040.1995.tb00628.x

Li G, Lin L, Dong Y, An D, Li Y, Luo W, Yin X, Li W, Shao J, Zhou Y, Dai J, Chen W, Zhao C (2012) Testing two models for the estimation of leaf stomatal conductance in four greenhouse crops cucumber, chrysanthemum, tulip and lilium. *Agricultural and Forest Meteorology* **165**, 92–103. doi:10.1016/j.agrformet.2012.06.004

Lobell DB, Hammer GL, Chenu K, Zheng B, McLean G, Chapman SC (2015) The shifting influence of drought and heat stress for crops in northeast Australia. *Global Change Biology* **21**, 4115–4127. doi:10.1111/gcb.13022

Long SP, Marshall-Colon A, Zhu X-G (2015) Meeting the global food demand of the future by engineering crop photosynthesis and yield potential. *Cell* **161**, 56–66. doi:10.1016/j.cell.2015.03.019

Ludlow MM (1981) Effect of temperature on light utilization efficiency of leaves in C_3 legumes and C_4 grasses. *Photosynthesis Research* **1**, 243–249. doi:10.1007/BF00034267

Massad R-S, Tuzet A, Bethenod O (2007) The effect of temperature on C_4-type leaf photosynthesis parameters. *Plant, Cell & Environment* **30**, 1191–1204. doi:10.1111/j.1365-3040.2007.01691.x

Massignam AM (2003) Quantifying nitrogen effects on crop growth processes in maize and sunflower. PhD thesis. School of Land, Crop and Food Sciences, University of Queensland, St Lucia, Qld, Australia.

Monsi M, Saeki T (1953) Über den Lichtfaktor in den Pflanzengesellschaften und seine Bedeutung für die Stoffproduktion. *Japanese Journal of Botany* **14**, 22–52.

Muchow RC, Sinclair TR (1994) Nitrogen response of leaf photosynthesis and canopy radiation use efficiency in field-grown maize and sorghum. *Crop Science* **34**, 721–727. doi:10.2135/cropsci1994.0011183X003400030022x

Nagai T, Makino A (2009) Differences between rice and wheat in temperature responses of photosynthesis and plant growth. *Plant & Cell Physiology* **50**, 744–755. doi:10.1093/pcp/pcp029

O'Leary GJ, Christy B, Nuttall J, Huth N, Cammarano D, Stöckle C, Basso B, Shcherbak I, Fitzgerald G, Luo Q, Farre-Codina I, Palta J, Asseng S (2015) Response of wheat growth, grain yield and water use to elevated CO_2 under a free-air CO_2 enrichment (FACE) experiment and modelling in a semi-arid environment. *Global Change Biology* **21**, 2670–2686. doi:10.1111/gcb.12830

Olson SN, Ritter K, Rooney W, Kemanian A, McCarl BA, Zhang Y, Hall S, Packer D, Mullet J (2012) High biomass yield energy sorghum: developing a genetic model for C_4 grass bioenergy crops. *Biofuels, Bioproducts & Biorefining* **6**, 640–655. doi:10.1002/bbb.1357

Parton WJ, Logan JA (1981) A model for diurnal variation in soil and air temperature. *Agricultural Meteorology* **23**, 205–216. doi:10.1016/0002-1571(81)90105-9

Pons TL, Flexas J, von Caemmerer S, Evans JR, Genty B, Ribas-Carbo M, Brugnoli E (2009) Estimating mesophyll conductance to CO_2: methodology, potential errors, and recommendations. *Journal of Experimental Botany* **60**, 2217–2234. doi:10.1093/jxb/erp081

Reyenga PJ, Howden SM, Meinke H, McKeon GM (1999) Modelling global change impacts on wheat cropping in south-east Queensland, Australia. *Environmental Modelling & Software* **14**, 297–306. doi:10.1016/S1364-8152(98)00081-4

Sands P (1995) Modelling Canopy Production. II. From single-leaf photosynthesis parameters to daily canopy photosynthesis. *Functional Plant Biology* **22**, 603–614.

Sellers PJ, Berry JA, Collatz GJ, Field CB, Hall FG (1992) Canopy reflectance, photosynthesis, and transpiration. 3. A reanalysis using improved leaf models and a new canopy integration scheme. *Remote Sensing of Environment* **42**, 187–216. doi:10.1016/0034-4257(92)90102-P

Sharkey TD, Bernacchi CJ, Farquhar GD, Singsaas EL (2007) Fitting photosynthetic carbon dioxide response curves for C_3 leaves. *Plant, Cell & Environment* **30**, 1035–1040. doi:10.1111/j.1365-3040.2007.01710.x

Sharwood RE, Ghannoum O, Whitney SM (2016) Prospects for improving CO_2 fixation in C_3-crops through understanding C_4-Rubisco biogenesis and catalytic diversity. *Current Opinion in Plant Biology* **31**, 135–142. doi:10.1016/j.pbi.2016.04.002

Sinclair TR, Horie T (1989) Leaf nitrogen, photosynthesis, and crop radiation use efficiency – a review. *Crop Science* **29**, 90–98. doi:10.2135/cropsci1989.0011183X002900010023x

Sinclair TR, Muchow RC (1999) Radiation use efficiency. *Advances in Agronomy* **65**(65), 215–265. doi:10.1016/S0065-2113(08)60914-1

Tubiello F, Volk T, Bugbee B (1997) Diffuse light and wheat radiation-use efficiency in a controlled environment. *Life Support & Biosphere Science* **4**, 77–85.

van Oosterom EJ, Borrell AK, Chapman SC, Broad IJ, Hammer GL (2010) Functional dynamics of the nitrogen balance of sorghum: I. N demand of vegetative plant parts. *Field Crops Research* **115**, 19–28. doi:10.1016/j.fcr.2009.09.018

von Caemmerer S (2000) 'Biochemical models of leaf photosynthesis. Vol. 2.' (CSIRO Publishing: Melbourne)

von Caemmerer S (2013) Steady-state models of photosynthesis. *Plant, Cell & Environment* **36**, 1617–1630. doi:10.1111/pce.12098

Vos J, Evers JB, Buck-Sorlin GH, Andrieu B, Chelle M, de Visser PHB (2010) Functional–structural plant modelling: a new versatile tool in crop science. *Journal of Experimental Botany* **61**, 2101–2115. doi:10.1093/jxb/erp345

Wong SC, Cowan IR, Farquhar GD (1979) Stomatal conductance correlates with photosynthetic capacity. *Nature* **282**, 424–426. doi:10.1038/282424a0

Wu A, Song Y, van Oosterom EJ, Hammer GL (2016) Connecting biochemical photosynthesis models with crop models to support crop improvement. *Frontiers in Plant Science* **7**, 1518. doi:10.3389/fpls.2016.01518

Yan W, Hunt LA (1999) An equation for modelling the temperature response of plants using only the cardinal temperatures. *Annals of Botany* **84**, 607–614. doi:10.1006/anbo.1999.0955

Yin X, Struik PC (2008) Applying modelling experiences from the past to shape crop systems biology: the need to converge crop physiology and functional genomics. *New Phytologist* **179**, 629–642. doi:10.1111/j.1469-8137.2008.02424.x

Yin X, Struik PC (2009) C_3 and C_4 photosynthesis models: an overview from the perspective of crop modelling. *NJAS Wageningen Journal of Life Sciences* **57**, 27–38. doi:10.1016/j.njas.2009.07.001

Yin X, van Laar HH (2005) 'Crop systems dynamics: an ecophysiological simulation model for genotype-by-environment interactions.' (Wageningen Academic Publishers: Wageningen, The Netherlands)

Zhang H, Nobel P (1996) Dependency of C_i/C_a and leaf transpiration efficiency on the vapour pressure deficit. *Functional Plant Biology* **23**, 561–568.